Scientia Horticulturae 352 (2025) 114425

Contents lists available at ScienceDirect

Scientia Horticulturae

journal homepage: www.elsevier.com/locate/scihorti

Research Paper

Yield estimation based on agronomic traits in vegetables under different biochar levels

Dennis Ccopi *, Edilson Requena-Rojas, Alberto Arias-Arredondo, Maglorio Taipe, Jhonny Marcelo, Samuel Pizarro

Estación Experimental Agraria Santa Ana, Dirección De Servicios Estratégicos Agrarios, Instituto Nacional de Innovación Agraria (INIA), Carretera Saños Grande - Hualahoyo Km 8 Santa Ana, Huancayo, Junín 12006, Peru

ARTICLE INFO

Keywords:
Biochar
Vegetables
Machine learning
Spectral indices
Sustainable agriculture
Yield prediction

ABSTRACT

Biochar, a carbon-rich material produced through oxygen-limited pyrolysis of organic biomass, demonstrates exceptional potential as a soil amendment due to its porous structure and stability. This research investigated the impact of guinea pig manure biochar on three vegetable species cultivated in high Andean conditions: spinach (*Spinacia oleracea L.*), cabbage (*Brassica oleracea var.*), and chard (*Beta vulgaris var.*). The study implemented four biochar application rates (0, 10, 20, and 30 t/ha) and measured comprehensive agronomic parameters including leaf count, leaf length, and fresh/dry biomass of both leaves and roots. Simultaneously, UAV-captured multispectral imagery provided spectral indices that were integrated with agronomic data into machine learning models: linear regression, support vector machines (SVM), and regression trees (CART). Results demonstrated significant vegetative growth enhancement and yield increases across all crops, with the 30 t ha^{-1} application rate producing optimal outcomes. Predictive modeling exhibited remarkable accuracy: spinach analysis via SVM achieved $R^2 = 0.94$ and RMSE = 0.32 g; chard analysis through CART delivered $R^2 = 0.92$ and RMSE = 0.35 g; and cabbage assessment using CART yielded $R^2 = 0.91$ and RMSE = 0.38 g. This research substantiates biochar's effectiveness as an organic amendment while establishing a reliable framework for crop yield prediction using machine learning algorithms integrated with spectral data. These findings position biochar as a valuable component in sustainable agricultural systems, particularly for vegetable production in challenging high-altitude environments.

1. Introduction

By 2050, the global population is projected to exceed 9 billion people (Nassary, 2025), creating an urgent need for sustainable food production systems that can withstand climate change, soil degradation, and water scarcity (Luna-Garcia et al., 2023). Optimizing both crop productivity and nutritional quality has become critical in addressing growing food insecurity concerns (Hernández-huerta et al., 2025).

Vegetables are essential components of agri-food systems due to their exceptional nutrient density and vital contribution to healthy diets (Knez et al., 2024). Leafy greens such as *Spinacia* oleracea L. (spinach), *Brassica oleracea* varieties (cabbage), and *Beta vulgaris* varieties (chard) are particularly valuable for their rich content of vitamins (A, C and K), minerals (iron, calcium), and bioactive compounds with potent antioxidant properties (Isaza et al., 2025; Wang et al., 2025).

Beyond enhancing food security, efficient cultivation of these nutrient-dense crops directly addresses malnutrition challenges, establishing them as foundational elements of resilient and sustainable agricultural systems worldwide (Sharma et al., 2021).

In recent years, biochar has emerged as a promising organic soil amendment that offers sustainable alternatives for agricultural production while preserving soil health and environmental integrity (Ren et al., 2025). This carbon-rich material not only helps sequester carbon and mitigate climate change impacts through resilient farming systems (Garcia et al., 2025), but also significantly reduces farmers' dependence on costly synthetic fertilizers (Nassary, 2025).

Biochar is produced through the process of pyrolysis—the thermochemical decomposition of organic biomass at elevated temperatures (400–700 °C) under oxygen-limited conditions (H. Liu et al., 2025). This controlled transformation creates a highly porous, recalcitrant carbon structure with unique physicochemical properties. When incorporated into soil, biochar enhances critical parameters including: aeration,

* Corresponding author.
E-mail address: dennisccopit@gmail.com (D. Ccopi).

https://doi.org/10.1016/j.scienta.2025.114425
Received 15 April 2025; Received in revised form 22 September 2025; Accepted 29 September 2025
Available online 6 October 2025

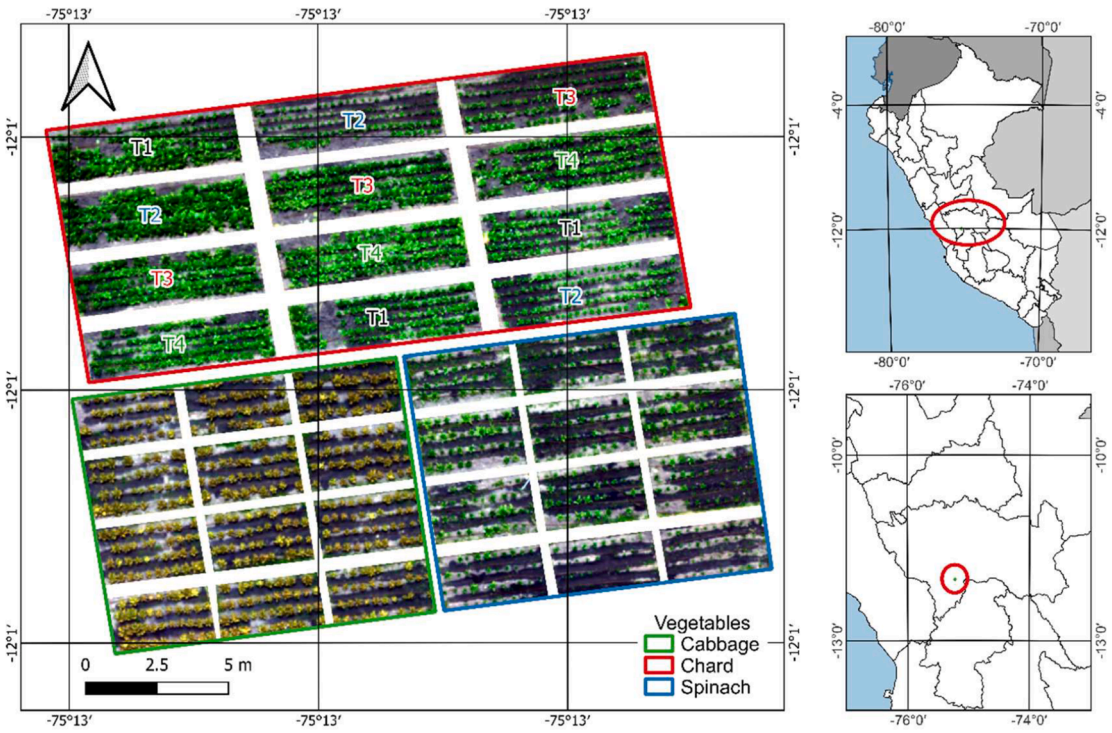

Fig. 1. Location of the field experiment and experimental design chard, spinach and cabbage in Santa Ana.

water-holding capacity, cation exchange capacity, and stable organic carbon content (Guo et al., 2025). Furthermore, biochar serves as a favorable habitat for beneficial soil microorganisms, creating diverse microbial communities that enhance nutrient cycling and availability for plant uptake (Yan et al., 2025).

Among the various soil amendments available, manure-derived biochar stands out for its exceptional ability to improve phosphorus availability and enhance nutrient retention, positioning it as a promising sustainable biological amendment with significant agricultural potential (Taweengern et al., 2025). These properties not only increase soil fertility but also demonstrably support crop growth and yield, as confirmed by recent field studies across diverse agricultural contexts (Eghlima et al., 2025; Karlsson et al., 2025). Due to these documented benefits, its adoption has expanded globally, particularly in regions seeking sustainable approaches to improve soil quality and boost agricultural productivity (Lin et al., 2025; Y. Liu et al., 2025). However, important questions persist regarding its direct impacts on specific crop quality parameters and yield consistency, as well as the underlying mechanisms that determine its effectiveness across different soil types, climate conditions, and management systems (Marazza et al., 2022). Despite compelling evidence associating manure-derived biochar with improved soil fertility indicators, these uncertainties have sparked rigorous scientific debate, highlighting the critical need for more targeted research to fully define its agronomic scope and optimize application protocols in sustainable agriculture (Gelardi et al., 2025; Yan et al., 2025).

The integration of biochar as a soil amendment represents a critical agronomic parameter requiring systematic monitoring due to its substantial influence on water retention capacity, soil fertility enhancement, and subsequent crop productivity outcomes. Traditional methodologies for quantifying agronomic traits have demonstrated significant limitations, including labor intensiveness, temporal inefficiency, and susceptibility to human-induced measurement errors (Bazrafkan et al., 2025). This methodological gap has catalyzed the development and implementation of proximal remote sensing technologies and photogrammetric approaches, further augmented by artificial intelligence (AI) algorithms that facilitate sophisticated data processing capabilities and enable the construction of high-precision predictive models for comprehensive agricultural assessment (Song et al., 2024; Xue et al., 2025).

The agricultural sector has undergone substantial transformation through the deployment of unmanned aerial vehicles (UAVs), which have fundamentally revolutionized precision agriculture paradigms by enabling intelligent, time-sensitive farming interventions (Zhang et al., 2025).. This technological advancement has been complemented by the integration of machine learning (ML) frameworks (Dayil et al., 2025) that support near real-time yield estimation protocols (Gade et al., 2025), thereby optimizing agricultural management strategies and enhancing evidence-based decision-making processes across diverse farming systems (Cao et al., 2025).

This research evaluates the efficacy of biochar amendments in the cultivation of three economically significant leafy greens: spinach (*Spinacia oleracea* L.), cabbage (*Brassica oleracea* var. *capitata*), and chard (*Beta vulgaris* subsp. *vulgaris*). Additionally, the study develops robust yield prediction models by integrating remote sensing-derived spectral indices, quantifiable agronomic parameters, and advanced machine learning algorithms. The resulting predictive frameworks will facilitate precise yield estimation in biochar-amended cropping systems while simultaneously enabling optimization of management practices according to site-specific agricultural conditions. This multidisciplinary approach addresses critical gaps in precision agriculture by providing data-driven decision support tools that enhance resource efficiency, promote sustainable cultivation practices, and enable context-sensitive agronomic interventions across diverse production environments.

2. Materials and methods

2.1. Description of the study area

The Santa Ana Experimental Station, managed by the National Institute of Agricultural Innovation (INIA), is located in the central Andes of Peru, in the province of Huancayo, Junín department (Fig. 1), at an approximate altitude of 3250 m.a.s.l. The area has a temperate cold climate, with an average annual temperature of 11 °C and average

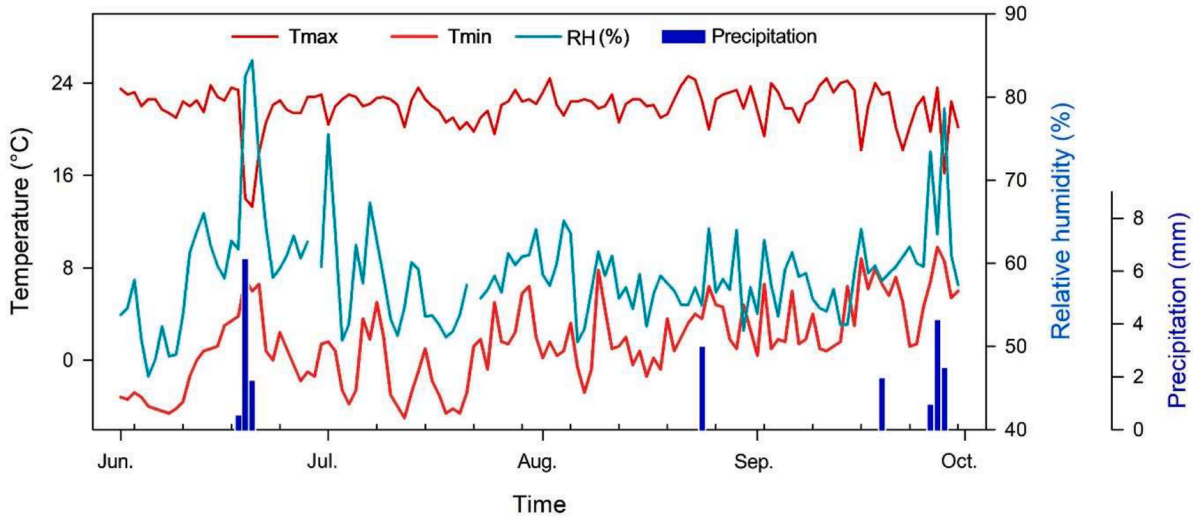

Fig. 2. Santa Ana meteorological station – SENAMHI. Daily data.

Table 1
Chemical characteristics of the soil and biochar.

	pH	CE (mS m^{-1})	OM (%)	P (mg kg^{-1})	K (mg kg^{-1})
Soil	7.0	0.12	4.4	83.8	295
Biochar	8.4	6.29	40.4	21,910.0	31,034.0

pH = potential hydrogen; CE = electrical conductivity; OM= organic matter; *P* = phosphorus content and *K* = potassium content.

annual precipitation ranging from 700 to 1200 mm, mainly concentrated between October and April (Senamhi, 2020; Ccopi et al., 2024). According to data from the Santa Ana meteorological station operated by Senamhi, located 250 m from the experimental site, daily weather variations between June and September showed maximum temperatures ranging from 13.3 to 24.6 °C, and minimum temperatures from −5 to 9.8 °C. Relative humidity ranged between 46.4 and 86.4 %, while daily precipitation reached up to 6.5 mm (Fig. 2).

2.2. Soil, biochar, vegetables and experimental design

Guinea pig manure was collected, sieved to ensure uniformity, and subsequently air-dried for 72 h until achieving a moisture content of approximately 20 %, which has been demonstrated to enhance pyrolysis process efficiency (Mishra et al., 2025). The pyrolysis procedure was conducted using a fixed-bed reactor system following slow pyrolysis protocols as described by (T.-J. Jiang et al., 2024). Thermal treatment was maintained at temperatures ranging from 350 to 400 °C for a duration of 4 h (Jha et al., 2023; Santos et al., 2025), followed by a controlled cooling period of 2 h (Qayyum et al., 2020). This process yielded biochar at a conversion efficiency of 35 %. The experimental soil was classified as loam textured, consisting of 40 % sand, 37 % silt, and 22 % clay fractions. The physicochemical properties of both the soil substrate and the produced biochar are comprehensively presented in Table 1.

Seeds of spinach (*Spinacia oleracea*), chard (*Beta vulgaris*), and cabbage (*Brassica oleracea*) were procured from a local commercial nursery. The experiment employed a Completely Randomized Design (CRD) with four discrete biochar application treatments: T1 (0 t ha^{-1}, serving as control), T2 (10 t ha^{-1}), T3 (20 t ha^{-1}), and T4 (30 t ha^{-1}). Each treatment was replicated three times and randomly assigned to experimental plots, as depicted in Fig. 1. This rigorous experimental design facilitated the systematic evaluation of varying biochar application rates on vegetable development while mitigating experimental variability through the randomization of experimental units across the study area.

2.3. Methodological process

Fig. 3 illustrates the study's methodological framework, comprising four interconnected phases. Initially, treatments utilizing biochar derived from guinea pig manure were administered to experimental plots. Subsequently, agronomic parameters of the crops were assessed concurrently with the acquisition of multispectral imagery via unmanned aerial vehicles (UAVs) during a single diurnal period. The third phase entailed comprehensive processing of the acquired imagery to extract multiple spectral indices. The final phase involved the implementation of machine learning algorithms to integrate the spectral indices with agronomic data, thereby enabling accurate prediction of crop yield potential.

2.4. Recording and evaluation of agronomic traits

Sowing was carried out on June 9, 2024, followed by systematic weekly agronomic assessments from July 4 to September 19 (covering 102 days after sowing, DAS). Data collection was performed at regular 7-day intervals (25, 32, 39, 46, 53, 60, 67, 74, 81, 88, 95, and 102 DAS). During this monitoring period, multiple parameters were evaluated in chard, spinach, and cabbage, including: leaf number per plant (NO), horizontal and vertical leaf dimensions (LW and LVH, in cm), leaf height (LFH, in cm), aphid infestation incidence (%), and insect-mediated foliar damage (%). Leaf dimensions (LW, LVH, and LFH) were measured using a ruler graduated in centimeters, while leaf number (NO), aphid incidence, and foliar damage (%) were recorded on field sheets through direct observation.

Furthermore, comprehensive biomass evaluations were conducted at three critical developmental stages (32, 67, and 102 DAS), encompassing both aerial and root components. These evaluations quantified fresh leaf weight (FLW, g), leaf dry weight (DLW, g), root system length (RL, cm), root fresh weight (FRW, g), and root dry weight (DRW, g).

Weight measurements (FLW, DLW, FRW, and DRW) were performed using an analytical balance (g). For dry weight determination, samples were oven-dried at 60 °C for 48 h. Root system length (RL) was measured with a ruler graduated in centimeters. This evaluation protocol enabled detailed monitoring of plant physiological development and allowed robust statistical analysis of treatment effects on biomass accumulation dynamics.

2.5. Recording and evaluation of multispectral data

Multispectral imagery acquisition was executed utilizing a DJI

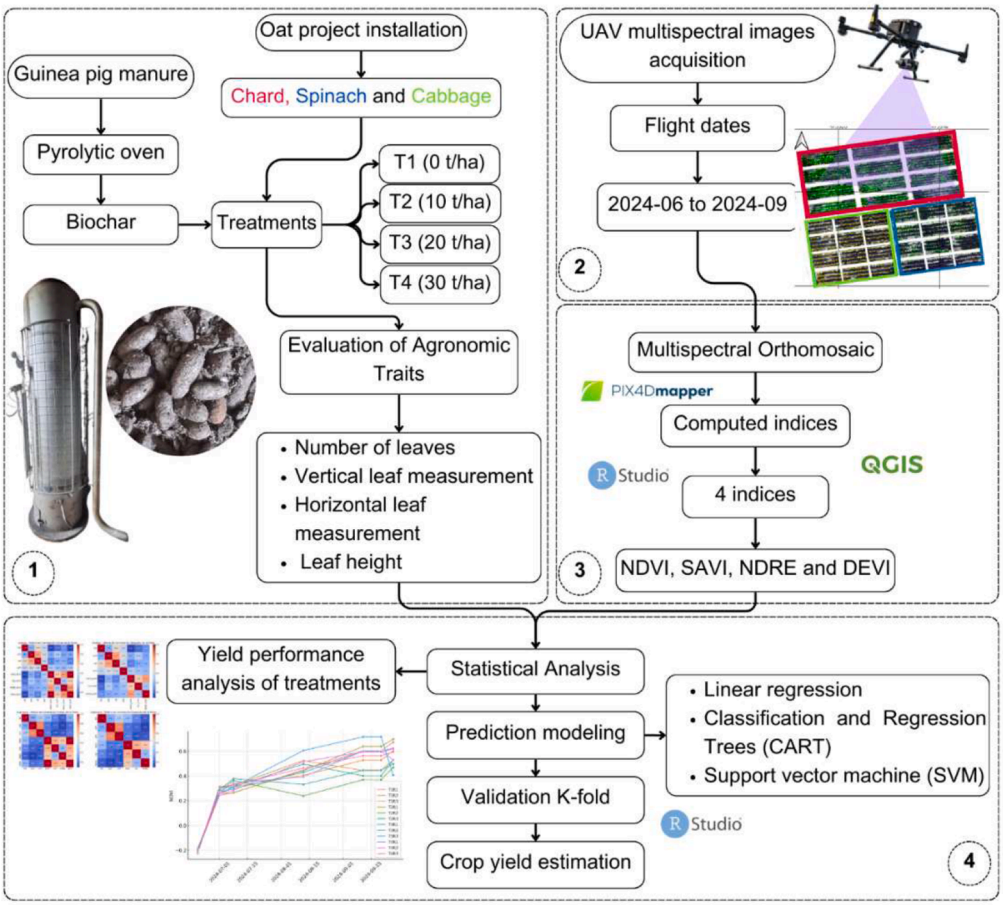

Fig. 3. Methodological approach of the study.

Table 2
Summary of spectral indices used for vegetation remote sensing.

Spectral index	Equation	Description
SAVI	$\frac{NIR - RED}{NIR + RED + L} x\ (1 + L)$	Soil-Adjusted Vegetation Index (SAVI). Corrects for soil influence in areas with low vegetation cover. L is an adjustment factor (commonly 0.5) (Huete, 1988).
NDVI	$\frac{NIR - RED}{NIR + RED}$	Normalized Difference Vegetation Index (NDVI). Measures of vegetation, health and vigor based on near infrared and red reflectance (Liu and Huete, 1995).
NDRE	$\frac{NIR - RE}{NIR + RE}$	Normalized Difference Red Edge Index (NDRE). Like NDVI, but it uses the red edge band, which is more sensitive to variations in chlorophyll content and early signs of plant stress (Davidson et al., 2022).
DEVI	$\frac{2\ x\ NIR - RED - BLUE}{2\ x\ NIR + RED + BLUE}$	Difference Enhanced Vegetation Index (DVI). Enhances sensitivity in vegetation detection and reduces atmospheric effects. (Jiang et al., 2008).

Matrice 300 RTK unmanned aerial vehicle (UAV) equipped with a MicaSense RedEdge-M multispectral sensor array. To ensure exceptional geospatial precision, a DJI D-RTK2 Mobile Station GNSS receiver was deployed, providing real-time kinematic corrections through advanced RTK technology. Aerial surveys were systematically conducted between 12:00 and 13:00 pm. at a standardized operational altitude of 30 m above ground level (AGL), implementing optimized technical parameters: image capture frequency at 2.1 s intervals, 80 % frontal and lateral overlap, and data preservation in high-fidelity 16-bit .tiff format. Ground control points (GCPs) were strategically positioned throughout the experimental site to facilitate precise georeferencing and spatial calibration. During flight operations, the UAV maintained a consistent velocity of 3 m s^{-1}, executing each pre-programmed flight plan in approximately 2 min. Subsequent photogrammetric processing was performed using Pix4D Pro Mapper software, generating high-resolution orthomosaic imagery with a Ground Sampling Distance (GSD) of 3 cm.

Data collection missions were strategically scheduled at 11, 25, 32, 67, 95, and 102 DAS, corresponding to critical phenological stages throughout crop development. This temporal sampling framework enabled comprehensive analysis of spatiotemporal variations, facilitating the identification of growth patterns and accurate assessment of vegetable crop responses to the experimental treatments. Following image acquisition and processing, multiple spectral indices were calculated (Table 2), selected based on their established relationships with vegetation vigor and their utility as proxies for physiological responses associated with photosynthetic activity (Legates and McCabe, 1999).

2.6. Predictive models

Crop yield prediction, quantified in grams per plant, was optimized through the implementation of sophisticated machine learning models that integrate both agronomic parameters and multispectral indices. These advanced computational techniques facilitate the identification of complex, non-linear patterns and significantly enhance analytical precision, thereby transcending the inherent limitations of conventional methodologies such as traditional statistical models and field-based visual assessments (Jabed and Azmi Murad, 2024). The progressive adoption of machine learning (ML) frameworks has catalyzed a

paradigm shift toward more intelligent, adaptive precision agriculture systems, enabling data-driven decision-making processes specifically calibrated to dynamic crop conditions in real-time environments (Morshed et al., 2025).

The Classification and Regression Trees (CART) algorithm represents a robust supervised learning methodology that constructs hierarchical decision trees to classify categorical data or predict continuous variables. In contemporary agricultural research, CART has emerged as an invaluable analytical tool within precision agriculture frameworks, particularly for accurate yield forecasting applications. Recent empirical studies have successfully deployed CART algorithms across diverse crop systems including maize, sugar beet, and soybean, capitalizing on its capacity to identify influential predictor variables in a transparent, interpretable, and visually intuitive manner. Furthermore, its rule-based structural architecture and inherent resilience against noisy or incomplete datasets render it exceptionally well-suited for agricultural applications characterized by high environmental variability (Ansarifar et al., 2021; Jhajharia and Mathur, 2023; Trentin et al., 2024).

Conversely, the Support Vector Machine (SVM) algorithm addresses both classification and regression challenges through fundamentally different mechanisms. Its methodological approach centers on identifying the optimal hyperplane that maximizes the margin between data categories, employing kernel transformations to effectively model complex non-linear relationships within multidimensional feature spaces (Lepnaan Dayil et al., 2025). This capacity for non-linear function approximation positions SVM as particularly valuable for agricultural systems characterized by complex interactions between biotic and abiotic factors.

Multiple linear regression was deliberately incorporated as a baseline comparative model, selected for its algorithmic simplicity and high degree of interpretability. This conventional statistical approach maintains significant utility for estimating agricultural yield based on climatological variables, agronomic management interventions, and edaphic properties across diverse production (Morán-Figueroa et al., 2024; Picado and Romero, 2025). The inclusion of this traditional model facilitates quantitative assessment of the incremental predictive advantages conferred by more sophisticated machine learning architectures in agricultural yield forecasting applications.

For the CART implementation, systematic hyperparameter optimization was conducted across multiple configurations, including complexity parameter (cp) values ranging from 0.001 to 0.05, and maximum tree depth constraints between 1 and 10 levels. The SVM model underwent exhaustive grid search optimization, evaluating cost parameters between 0.1 and 50, gamma coefficients between 0.001 and 0.1, and epsilon values between 0.01 and 1. This comprehensive validation and hyperparameter tuning methodology enabled rigorous inter-model performance comparison while identifying optimal configurations for maximizing crop yield prediction accuracy.

2.7. Statistical analysis and K-fold cross-validation

The R statistical environment was employed for comprehensive data processing and analysis throughout this investigation. Data management procedures utilized the readxl, dplyr, and tidyr packages (Wickham et al., 2024) for preprocessing and cleaning operations, while visualization and correlation analyses were conducted via ggplot2, corrplot, and psych packages (Levy, 2024). Distributional assumptions were rigorously evaluated through the Shapiro-Wilk normality test, complemented by Levene's test for homogeneity of variances. Dimensionality reduction through Principal Component Analysis (PCA) was executed using the FactoMineR and factoextra packages (Husson et al., 2025).

For machine learning model development and validation, the caret, rpart, and e1071 packages were implemented (Grandgirard et al., 2002; Max et al., 2024). A robust K-fold cross-validation framework was established with the dataset stratified into five equivalent partitions to ensure methodologically sound performance evaluation across algorithms. During each iterative validation cycle, one partition served as the test set while the remaining four partitions constituted the training corpus, thereby ensuring complete utilization of all observations across both training and evaluation phases (Hidayaturrohman, 2025; Villegas-camacho et al., 2025).

Table 3
Effect of treatments on chard development by DAS.

Variables	DAS	Treatments			
		T1	T2	T3	T4
LFH (cm)	25	6.7567 ± 1.6708a	6.2500 ± 1.6905a	6.9367 ± 1.5531a	6.7267 ± 1.4633a
	32	7.6233 ± 1.6923a	7.2900 ± 1.7932a	7.7033 ± 1.4001a	7.6667 ± 1.6875a
	67	13.1400 ± 3.8964ab	13.0300 ± 6.9488b	12.8367 ± 3.5328b	16.1800 ± 3.2397a
	95	22.1133 ±4.4493b	22.4400 ± 4.1095b	23.5667 ± 3.2645b	28.1200 ± 4.9225a
	102	27.3100 ± 4.1827b	26.1533 ± 4.4652b	27.5867 ± 3.5044b	33.6167 ± 5.7324a
LVH (cm)	25	3.7367 ± 0.8992c	3.2400 ± 0.8811bc	2.7033 ± 0.6505a	2.9400 ± 0.5727ab
	32	4.4367 ± 1.0354b	4.0567 ± 1.0650ab	3.4300 ± 0.6834a	3.7167 ± 0.5180ab
	67	9.4467 ± 2.9786ab	9.3567 ± 4.7747b	8.5900 ± 2.2377b	10.8600 ± 1.7379a
	95	17.5600 ± 2.9627b	19.0500 ± 2.6173b	19.7367 ± 2.8982b	24.0200 ± 3.8778a
	102	23.4933 ± 3.7111b	22.0533 ± 3.1749b	23.8767 ± 3.8392b	28.8300 ± 4.8187a
LW (cm)	25	1.8833 ± 0.4793a	2.1333 ± 0.6984a	1.7567 ± 0.4289a	1.9600 ± 0.4190a
	32	2.4167 ± 0.5193ab	2.6600 ± 1.0166ab	2.2033 ± 0.4507b	2.5600 ± 0.4048a
	67	7.1333 ± 1.9027b	6.8100 ± 2.7902b	6.9900 ± 1.6076b	8.6233 ± 1.6627a
	95	11.8500 ± 2.7971c	12.6533 ± 2.2703bc	14.1600 ± 2.3906ab	14.9633 ± 1.7582a
	102	15.3767 ± 3.1654b	14.5267 ± 2.4239b	16.3600 ± 2.8392ab	17.1600 ± 2.0356a
NO (leaves/ plant)	25	4.2000 ± 0.8469b	4.9000 ± 1.0619a	4.7000 ± 0.9154ab	4.7667 ± 0.8172ab
	32	5.3667 ± 1.0662a	5.9667 ± 1.2172a	5.4667 ± 0.9371a	5.7333 ± 0.9072a
	67	10.2667 ± 1.8742ab	10.0000 ± 3.6199b	10.4000 ± 2.1432ab	11.7333 ± 2.1485a
	95	12.3333 ± 2.2642a	a12.3667 ± 3.4289	12.9000 ± 2.6438a	13.8667 ± 3.0256a
	102	12.9333 ± 2.3332ab	13.1667 ± 3.4550b	14.5000 ± 2.4740ab	14.8000 ± 2.8089a

Kruskal-Wallis test, followed by Bonferroni post hoc analysis for multiple comparisons ($p < 0.05$).

3. Results

3.1. Effects of biochar on agronomic traits and vegetable yield

3.1.1. Agronomic traits

Due to the non-normal distribution of variables, data were analyzed using the Kruskal-Wallis test, followed by Bonferroni post hoc analysis for multiple comparisons. In the results, different letters within the same row indicate statistically significant differences between treatments ($p < 0.05$). Table 3 presents the effects of experimental treatments on chard morphological development across four critical growth stages (25, 67, 95, and 102 DAS). Four key morphological parameters were evaluated: leaf number per plant (NO), vertical leaf length (LW), leaf height (LFH), and horizontal leaf length (LVH). At 25 DAS (early vegetative stage), significant differences emerged in foliar abundance, with treatment T2 exhibiting superior performance (4.90) compared to T1 (4.20), while T3 and T4 displayed intermediate values.

Table 4
Effect of treatments on spinach development by DAS.

Variables	DAS	Treatments			
		T1	T2	T3	T4
LFH (cm)	25	3.0500 ± 0.7763a	3.3733 ± 1.1323a	3.2167 ± 1.0120a	2.9633 ± 1.2813a
	32	3.5167 ± 0.9685a	3.2700 ± 1.1423a	3.4467 ± 1.0126a	3.7867 ± 1.6105a
	67	8.7733 ± 2.7142a	9.4200 ± 3.5254a	8.9033 ± 2.4214a	10.1333 ± 3.0441a
	95	14.5233 ± 2.3092c	16.300 ± 2.6392bc	17.9100 ± 3.8227b	21.6167 ± 2.7789a
	102	15.9367 ± 2.6089c	19.2100 ± 4.0528b	18.0233 ± 3.2714bc	23.3833 ± 2.8543a
LVH (cm)	25	2.6500 ± 0.5680a	2.7167 ± 0.6075a	2.7467 ± 0.6129a	2.5300 ± 0.9777a
	32	2.6400 ± 0.7347a	2.4233 ± 0.6907a	2.6700 ± 0.6904a	2.7433 ± 0.9361a
	67	6.5100 ± 2.0694a	6.5133 ± 2.6418a	6.2933 ± 1.7898a	7.2400 ± 2.4731a
	95	11.6000 ± 2.0062c	14.0633 ± 2.8845b	14.4533 ± 2.6604b	18.4133 ± 2.8946a
	102	13.0733 ± 2.4100c	15.1733 ± 3.0694bc	15.7867 ± 2.6952b	20.0067 ± 3.0601a
LW (cm)	25	1.5567 ± 0.3191a	1.5833 ± 0.3364a	1.5300 ± 0.4010a	1.4467 ± 0.4761a
	32	1.5067 ± 0.5508a	1.5167 ± 0.4914a	1.5933 ± 0.5356a	1.7533 ± 0.6590a
	67	3.6200 ± 1.1909a	3.9133 ± 1.4002a	3.9167 ± 1.1665a	4.3900 ± 1.4043a
	95	7.5167 ± 1.7177c	8.5133 ± 1.5355bc	9.1567 ± 1.8673b	10.5667 ± 1.5421a
	102	8.3167 ± 2.1174c	9.1767 ± 1.8384bc	9.9533 ± 2.1896ab	11.3500 ± 1.7222a
NO (leaves/ plant)	25	3.7667 ± 0.7279c	3.3667 ± 0.8899bc	3.0333 ± 0.6149ab	2.7333 ± 0.5833a
	32	4.3000 ± 0.6513a	4.2333 ± 0.6261a	4.2667 ± 0.7849a	4.4000 ± 0.8944a
	67	10.3000 ± 2.3067a	10.7667 ± 2.4870a	11.0000 ± 2.0342a	11.2667 ± 2.4626a
	95	16.3333 ± 3.2519a	16.4667 ± 2.7004a	16.5333 ± 2.7384a	17.9333 ± 2.9704a
	102	18.3333 ± 2.7585b	18.7667 ± 2.5688ab	19.2667 ± 3.0843ab	20.8000 ± 2.9525c

Kruskal-Wallis test, followed by Bonferroni post hoc analysis for multiple comparisons ($p < 0.05$).

Table 5
Effect of treatments on cabbage development by DAS.

Variables	DAS	Treatments			
		T1	T2	T3	T4
LFH (cm)	25	9.0333 ± 1.6983a	8.5800 ± 2.1723a	9.5433 ± 2.3652a	11.2567 ± 1.9294b
	32	11.3833 ± 2.2644a	10.6300 ± 2.2254a	10.2533 ± 2.0603a	11.1967 ± 2.0248a
	67	20.0700 ± 1.9252a	20.7600 ± 4.0334a	18.9433 ± 3.1914a	16.8500 ± 2.6387b
	95	27.5833 ± 2.3371a	26.6433 ± 2.7860a	22.4167 ± 2.1134b	21.8833 ± 1.6114b
	102	30.9967 ± 2.10720a	30.2767 ± 3.1427a	26.3967 ± 2.3709b	24.4167 ± 2.0910b
LVH (cm)	25	3.2967 ± 0.7531a	3.3833 ± 0.8714a	3.3733 ± 0.7777a	3.5733 ± 0.7216a
	32	3.9833 ± 0.8956a	3.9467 ± 0.7450a	4.0367 ± 0.5654a	4.3233 ± 0.8701a
	67	12.0100 ± 1.5479a	12.2133 ± 2.8034ab	11.1000 ± 2.0440ab	10.7033 ± 2.3271b
	95	20.3900 ± 2.2573a	20.4933 ± 2.3267a	17.8800 ± 1.7175b	18.1267 ± 1.7743b
	102	22.8800 ± 2.8920a	23.2000 ± 3.4811a	19.6800 ± 2.0615b	19.4633 ± 1.7101b
LW (cm)	25	2.3800 ± 0.4916a	2.2567 ± 0.5191a	2.3300 ± 0.4872a	2.5867 ± 0.4790a
	32	3.1100 ± 0.6413ab	2.7967 ± 0.4271a	2.8300 ± 0.3834ab	3.2100 ± 0.6053b
	67	10.4133 ± 1.5712ab	11.2400 ± 2.6532a	9.6467 ± 2.3825ab	9.6867 ± 2.5168b
	95	18.1667 ± 2.2220a	18.6533 ± 2.4568a	16.1300 ± 2.0110b	15.8000 ± 2.3647b
	102	19.7700 ± 2.3496a	20.7533 ± 2.9746a	17.6133 ± 2.3802b	17.2167 ± 2.713b
NO (leaves/ plant)	25	4.5333 ± 0.6288a	4.5667 ± 0.8976a	4.7000 ± 0.8769a	5.9333 ± 0.7849b
	32	6.7333 ± 0.9803ab	6.4667 ± 0.8996ab	6.4000 ± 1.0700a	7.2000 ± 1.0954b
	67	11.0333 ± 0.8899a	11.1000 ± 1.0619a	11.5000 ± 1.2247a	11.7000 ± 1.3429a
	95	16.6333 ± 2.0254a	15.5667 ± 1.1651ab	15.0000 ± 1.0828b	15.1333 ± 1.1366b
	102	19.8000 ± 1.7301a	17.8000 ± 1.1567b	16.3667 ± 0.9279c	16.2667 ± 1.0148

Kruskal-Wallis test, followed by Bonferroni post hoc analysis for multiple comparisons ($p < 0.05$).

For LVH, T1 demonstrated significantly greater development (3.73) compared to T3 (2.70) and T4 (2.94). Regarding vertical leaf dimensions (LW and LFH), T1 and T3 represented the maximum and minimum values respectively, with T1 consistently achieving superior results. By 67 DAS (mid-vegetative stage), treatment T4 exhibited the highest foliar abundance (11.73), followed by T1 and T3, while T2 demonstrated significantly reduced development (10.00). For vertical parameters (LW and LFH), T4 achieved maximum values (8.62 and 16.18, respectively), while T2 exhibited minimum values, indicating suboptimal growth under this treatment regime. At 95 DAS (pre-harvest stage), morphological parameters increased across all treatments, with T4 maintaining developmental superiority, particularly regarding LFH (22.44) and NO (13.00), while treatments T2 and T3 consistently displayed inferior performance across most evaluated parameters. By harvest (102 DAS), treatment T4 maintained statistically significant advantages across all morphological parameters: NO (12.53), LVH (28.83), and LFH (33.61), confirming its sustained positive effect on chard development throughout the cultivation cycle. Conversely, T2 consistently demonstrated inferior performance, with significantly reduced values for LVH (22.05) and LFH (26.15).

Table 4 illustrates the differential effects of experimental treatments on spinach morphological development throughout the growing season. During early development (25 DAS), foliar abundance (NO) was significantly higher in treatments T1 and T2 (3.77 and 3.67, respectively) compared to T3 and T4 (3.03 and 2.73). For horizontal leaf expansion (LVH), T1 demonstrated superior development (2.65), followed by T2, while T3 and T4 exhibited significantly reduced values. Vertical leaf width (LW) showed no significant variation across treatments. Regarding leaf height (LFH), T2 achieved maximum development (3.13), followed by T1, T3, and T4 in descending order.

By 32 DAS, no significant differences were observed in foliar abundance across treatments. Horizontal leaf expansion (LVH) was marginally higher in T2 (2.42) compared to T1 (2.64), though differences remained statistically insignificant. Vertical leaf width remained consistent across treatments. Leaf height was maximized in treatments T3 and T4. At mid-development (67 DAS), foliar abundance was numerically highest in T2 (10.77) and lowest in T1 (10.30), though without statistical significance. Horizontal leaf expansion (LVH) was significantly enhanced in T4 (4.39) compared to all other treatments. Similarly, T4 demonstrated superior vertical leaf width (6.24). Leaf height was maximized in T4 (10.13) and minimized in T1 (8.77).

During late vegetative development (95 DAS), T4 exhibited significantly higher foliar abundance (17.93) compared to T2 (14.47). Horizontal leaf expansion remained superior in T4 (14.81). Both vertical leaf width and leaf height were maximized in T4, with statistically significant advantages over all other treatments. At harvest maturity (102 DAS), treatment T4 consistently demonstrated superior performance across all morphological parameters: foliar abundance (20.07),

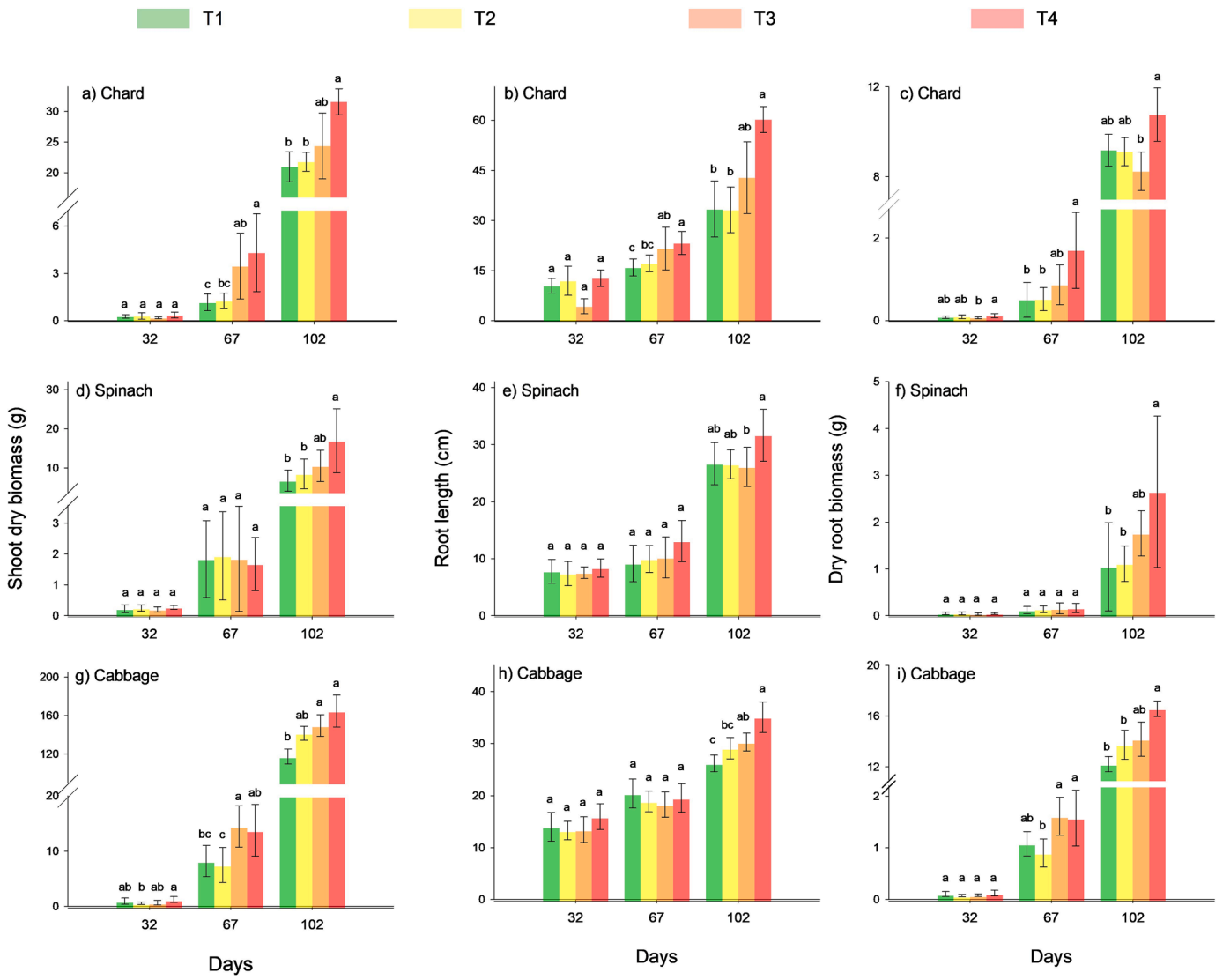

Fig. 4. Shoot dry biomass (a, d, g), root length (b, e, h), and dry root biomass (c, f, i) in chard, spinach, and cabbage grown at different biochar levels and days after sowing DAS. Bars represent mean ± SD. Different letters indicate significant differences ($p < 0.05$).

horizontal leaf expansion (11.35), vertical leaf width (11.35), and leaf height (23.38), with statistically significant advantages compared to all other treatments. Conversely, T1 consistently exhibited inferior performance across most parameters, particularly leaf height (15.94).

Table 5 illustrates the temporal influence of biochar treatments on cabbage morphological development across the complete growth cycle. During early developmental stages (25 and 32 DAS), no statistically significant differences were observed among treatments for any measured agronomic parameters, as evidenced by uniform statistical notation (a) across all treatments. During this initial growth phase, treatments T4 and T1 exhibited marginally superior performance, particularly regarding leaf height (LFH) and foliar abundance (NO), though these differences remained statistically insignificant.

By mid-vegetative development (67 DAS) and pre-heading stage (95 DAS), treatment effects became increasingly differentiated. At 67 DAS, treatments T3 and T2 demonstrated enhanced foliar development, with superior performance in leaf height and foliar abundance, while T1 exhibited comparatively reduced values. This developmental pattern persisted through 95 DAS, when treatments T3 and T4 achieved maximum values for leaf height and leaf width (LW), with T2 maintaining intermediate morphological development.

At harvest maturity (102 DAS), treatment differences manifested with statistical significance. Treatment T4 consistently demonstrated superior performance across nearly all morphological parameters, with particularly pronounced advantages in leaf height (31.00) and foliar abundance (19.90), indicating enhanced overall leaf development and potential photosynthetic capacity. Conversely, treatment T1 consistently exhibited significantly reduced morphological development across all measured parameters, reflecting substantially diminished growth potential throughout the cultivation cycle.

3.1.2. *Shoot biomass, root length, and root biomass*

Fig. 4 illustrates the differential effects of biochar treatments (T1–T4) on shoot dry biomass, root dry biomass, and root length across three horticultural crops (chard, spinach, and cabbage) measured at 32, 67, and 102 DAS. In chard (Figs. 4a–c), treatment T4 exhibited superior performance at 102 DAS, with statistically significant increases in both shoot biomass accumulation and root elongation compared to the control treatment (T1). For spinach cultivation (Figs. 4d–f), T4 similarly demonstrated enhanced efficacy, yielding significantly greater shoot and root biomass relative to both T1 and T2 treatments. This pattern of biomass enhancement was most pronounced at the final measurement interval. Cabbage specimens (Figs. 4g–i) responded most robustly to the T4 treatment, which generated consistently superior means across all

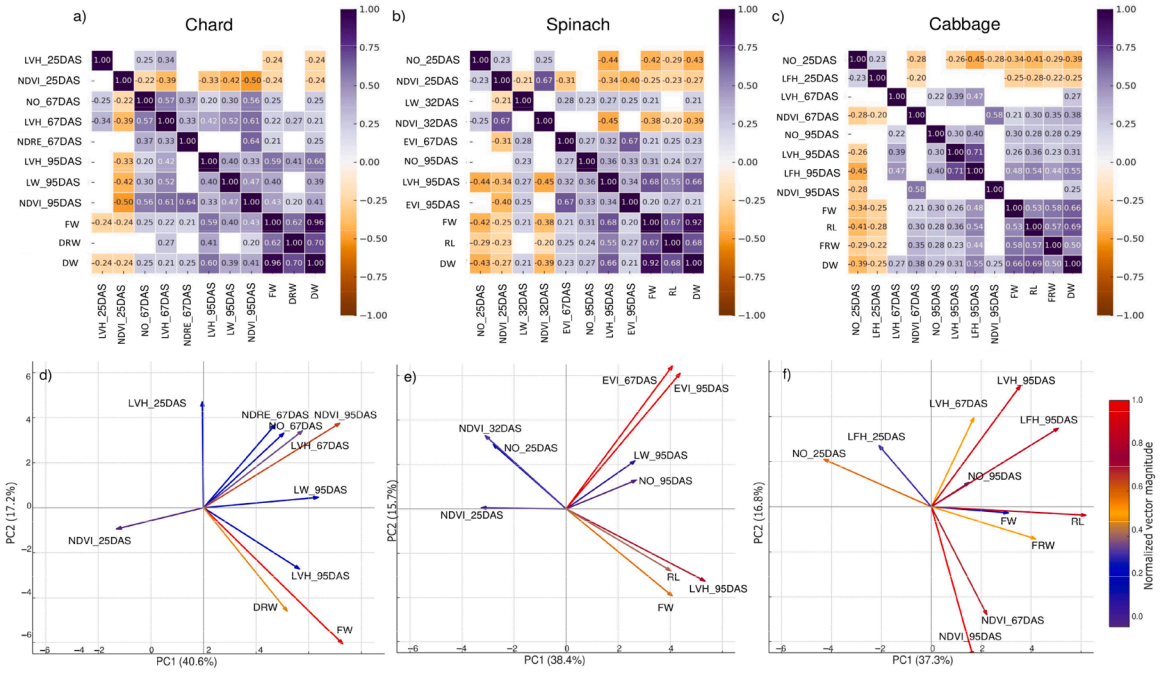

Fig. 5. Correlation matrices (a–c) and PCA biplots (d–f) of spectral indices and agronomic traits in chard (a, d), spinach (b, e), and cabbage (c, f).

evaluated parameters. Notably, significant differences between T4 and T1 were observed at all three temporal measurement points, indicating an early and sustained treatment effect. The analysis across all three horticultural species reveals that T4 consistently emerged as the most efficacious treatment, significantly enhancing both aerial vegetative development and root system architecture parameters throughout the cultivation period. These findings substantiate the dose-dependent physiological response of these crops to increasing biochar application rates, with marked improvements in biomass accumulation and root system development.

3.2. Yield prediction using agronomic covariates and multispectral information

3.2.1. Variable correlation

Fig. 5 shows the correlation matrices (a-c) and PCA (d-f) biplots integrating spectral, agronomic, and biomass variables in chard, spinach, and cabbage, considering dry weight (DW) as the variable of interest. In chard, indices measured at 25 DAS display weak correlations with DW, whereas at 67–95 DAS, NDVI and NDRE exhibit strong correlations. In spinach, EVI indices (67 and 95 DAS) show strong correlations with DW and root length, in contrast to the 25 DAS indices that present weak correlations. In cabbage, the association with DW is more stable throughout the cycle, although the 95 DAS indices show the strongest correlations.

The PCA biplots confirm these patterns, indicating that most of the variability in the three crops is explained by mid- and late-stage indices strongly correlated with DW. In chard, PC1 separates the 25 DAS indices, with weak correlations, from yield-related variables aligned with DW. In spinach, the 95 DAS indices are projected together with DW and root length, reinforcing their strong correlations. In cabbage, multiple indices (NDVI, NO, LVH, and LFH) contribute jointly, suggesting that DW estimation can benefit from integrating spectral information across different phenological stages.

3.2.2. Selection of prediction models

Fig. 6 shows the performance of the models across the three crops evaluated. In chard, all algorithms (MLR, SVM, and CART) achieved excellent fits (R^2 ranging from 0.89 to 0.97) with low error values, indicating high precision and stability in predictions. In spinach, MLR and SVM displayed lower generalization capacity (test R^2 between 0.64 and 0.70), while CART achieved better performance ($R^2 = 0.86$) with lower error, demonstrating greater adaptability. In cabbage, the results were more limited, as all models showed modest fits (R^2 between 0.65 and 0.79) and higher errors (RMSE ≈ 9–12), reflecting greater difficulty in accurately predicting this crop.

Based on model selection, Table 6 presents the tuned hyperparameters of the best-performing CART and SVM models, along with the estimated coefficients from the multiple linear regression (LR) model, used to predict dry shoot biomass dry yield in chard, spinach, and cabbage.

Chard and spinach shared a high cost (10.0) and low epsilon (0.01), suggesting a tighter fit; in contrast, cabbage was adjusted with a lower cost (5.0) and a more permissive epsilon (0.1). On the other hand, the multiple linear regression model included equations with coefficients for the selected predictive variables of DW. Chard and spinach shared the same mathematical expression, indicating a similar response to variables such as EVI_67DAS, EVI_95DAS, RL, FW, LW_32DAS, NO_95DAS, and LVH_95DAS. In contrast, the model for cabbage incorporated a larger number of variables, including NDVI_67DAS, NDVI_95DAS, LVH_67DAS, LFH_95DAS, and FRW, reflecting greater complexity in its growth dynamics and in explaining dry biomass yield.

3.2.3. Yield spatialization

Fig. 7 shows the spatial prediction of dry biomass yield (g m^2) for chard, spinach, and cabbage using the best-performing models for each case: CART for chard and cabbage, and SVM for spinach. Colors represent the magnitude of the predicted yield, with cool tones indicating lower values and warm tones indicating higher values. In all three crops, a clear increasing pattern in predicted dry biomass is observed as the biochar dose increases. Plots under T4 (30 t ha^{-1}) predominantly display red and orange tones, indicating high biomass levels, while T1 (0 t ha^{-1}) is associated with cooler colors such as blue and green, reflecting lower yields. This pattern remains consistent across chard, spinach, and cabbage, demonstrating the positive crop response to increasing biochar application in the soil.

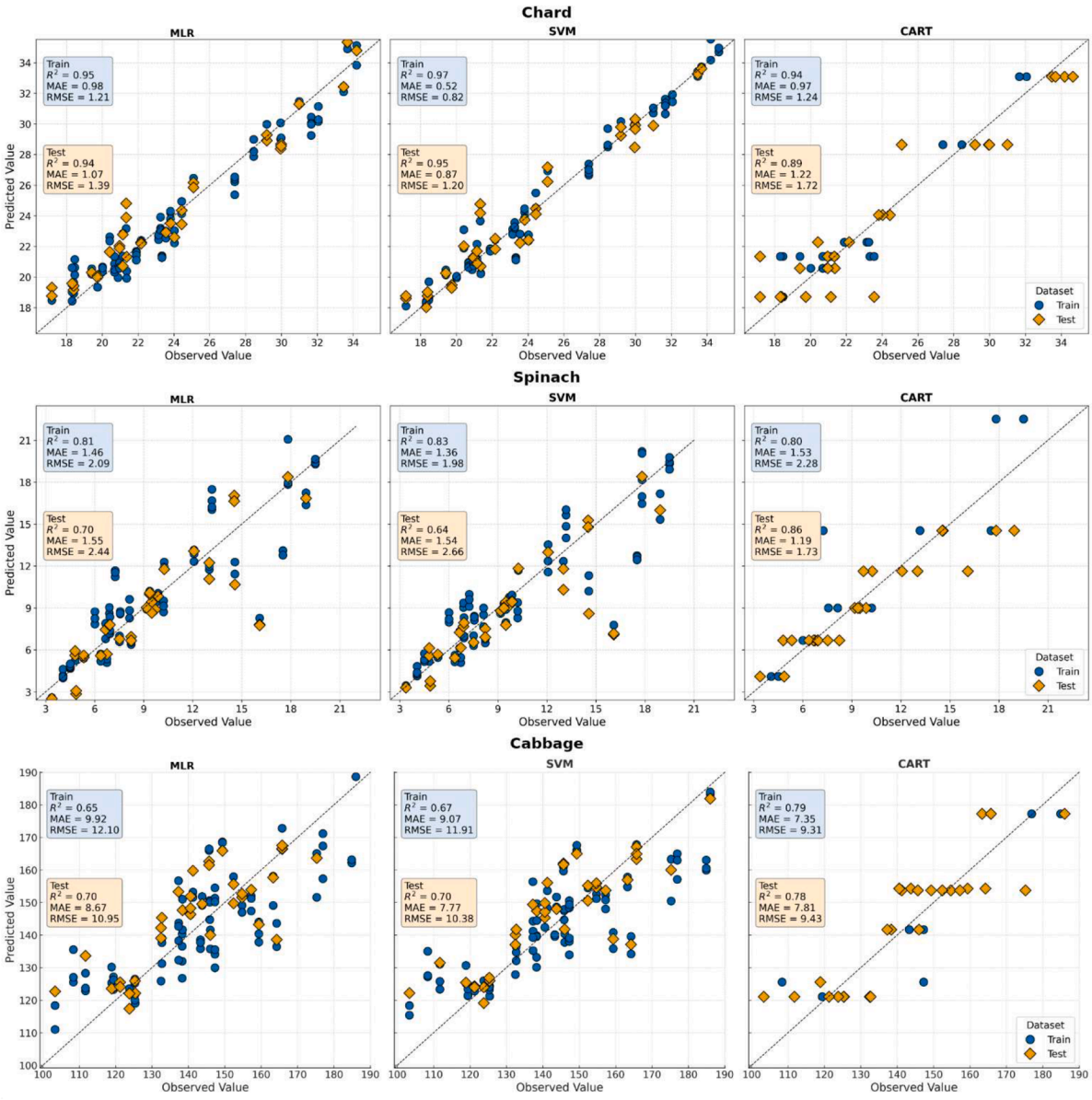

Fig. 6. Relationship between observed and predicted yield values for the MLR, SVM, and CART models in chard, spinach, and cabbage.

4. Discussion

The application of guinea pig manure-derived biochar demonstrated pronounced dose-dependent effects on vegetable crop productivity, with the highest application rate (30 t ha^{-1}, T4) consistently yielding superior morphological development and biomass accumulation across chard, spinach, and cabbage crops. Specifically, significant enhancements were observed in critical growth parameters including leaf height, foliar abundance, root system architecture, and both fresh and dry biomass (Table 3,4 and 5). These findings align with contemporary research documenting substantial improvements in crop productivity and soil physicochemical properties following biochar amendment, particularly within intensive agricultural systems and rotational cropping sequences (Hu et al., 2021; Canatoy et al., 2022).

At the physiological level, enhanced rhizospheric development was consistently observed across treatments, resulting in expanded nutrient absorption surface area and improved resource acquisition efficiency. This beneficial root architectural modification parallels effects documented in field investigations with cereal crops including maize and wheat (Xu et al., 2021). Notably, while application rates exceeding 30 t ha^{-1} have been investigated in previous studies, emerging research suggests potential threshold effects beyond this application rate, potentially inducing antagonistic responses regarding nutrient bioavailability and soil microbial community composition (Egbeagu et al., 2023).

In contrast to conventional research utilizing plant-derived biochar, this investigation employed biochar synthesized from guinea pig manure, presenting a regionally appropriate, sustainable amendment specifically tailored to agricultural systems in the central Andean region, where smallholder livestock production constitutes an integral component of rural livelihoods (Cárdenas, 2025). This localized approach exemplifies circular economy principles through strategic upcycling of readily available organic residues, thereby enhancing both technical feasibility and environmental sustainability (Ghazouani et al., 2023; Ortiz-Liébana et al., 2023). Furthermore, the observed agronomic responses suggest significant potential for biochar integration within low-input agricultural systems, potentially reducing dependence on synthetic fertilizers—an outcome consistent with contemporary research promoting biochar as a foundational component within resilient, ecologically sustainable agricultural frameworks (Hu et al., 2024;

Tabla 6
Hyperparameters of the Classification and Regression Tress (CART) and Support Vector Machine (SVM) models, and regression coefficients of the linear model for predicting dry biomass (DW) in chard, spinach, and cabbage.

Model	Chard	Spinach	Cabbage
CART	Cp = 0.001 maxdepth= 4	Cp = 0.001 maxdepth= 3	Cp = 0.021 maxdepth= 4
SVM	cost = 10.0, gamma = 0.01, epsilon = 0.01	cost = 10.0, gamma = 0.05, epsilon = 0.01	cost = 5.0, gamma = 0.005, epsilon = 0.1
MLR	DW = −4.937 + 0.1021xLW_32DAS + 7.8493 x EVI_67DAS + 1 × 10^{-4} x NO_95DAS + 0.1 x LVH_95DAS + (−1.2341) x EVI_95DAS + 0.1182 x FW + 0.1466 x RL	DW=−4.937+ 0.1021 x LW_32DAS + 7.8493 x EVI_67DAS + 1 × 10^{-4} x NO_95DAS + 0.1 x LVH_95DAS + (−1.2341) x EVI_95DAS + 0.1182 x FW + 0.1466 x RL	DW = −15.2039 + 1.2315 x LVH_67DAS +39.1811 x NDVI_67DAS + 0.4072 x NO_95DAS + −0.7863 x LVH_95DAS + 0.8334 x LFH_95DAS + 24.954 x NDVI_95DAS + 0.056 x FW + 1.7845 x RL + 0.0132 x FRW

Y. Jiang et al., 2024).

Various studies have demonstrated biochar's capacity to improve crop yield through modifications to soil physicochemical properties, enhanced nutrient availability, and increased water use efficiency. Abbruzzini et al. (2019) documented a 27 % increase in yield and 16 % increase in shoot biomass in wheat grown in tropical soils amended with sugarcane straw biochar, alongside a 71 % reduction in N2O emissions, highlighting both agronomic and environmental benefits. Gao et al. (2020) observed an average 18.8 % increase in plant water use efficiency following biochar application, emphasizing the importance of soil-climate conditions and biochar characteristics. Hall & Bell (2015) noted that in naturally low-fertility soils, such as sandy soils in southern Australia, biochar and compost application resulted in yield increases only during initial growing cycles, suggesting effects may be short-term without integrated fertilization and moisture management strategies.

The interaction between biochar and nutrients plays a critical role in its effectiveness. Canatoy et al. (2022) demonstrated biochar's ability to improve phosphorus efficiency by reducing fixation in acidic soils, while. Zhang et al. (2024) highlighted enhanced nitrogen efficiency through greater retention and improved synchronization with crop demand. Biochar has also shown significant capacity for immobilizing heavy metals, as noted by Xu et al. (2016), adding value to its application in degraded soils. However, response variability across crop types must be considered, as demonstrated by Zhang et al. (2020), where maize, beans, and sorghum exhibited different responses to biochar applications. The properties of biochar—including carbon content, alkalinity, and pyrolysis temperature—are fundamental determinants of its agronomic effects (Jaufmann et al., 2024; T.-J. Jiang et al. 2024). Overall, the literature indicates that biochar represents a promising strategy for enhancing agricultural productivity, provided it is integrated within sustainable and context-specific management systems.

In the present study (Figs. 4,5,6; Tables 3,4,5), machine learning algorithms—particularly Classification and Regression Trees (CART) and Support Vector Machine (SVM)—demonstrated remarkable effectiveness in predicting horticultural crop yields under varying biochar doses. These algorithms successfully identified complex patterns among agronomic variables including biomass, root length, and number leaf. This predictive capability aligns with Ye et al. (2024), whose research showed Random Forest algorithms outperforming traditional models in wheat and canola yield prediction by effectively handling nonlinear and high-dimensional data. Similarly, Ishaq et al. (2025) demonstrated that Convolutional Neural Network (CNN) and Long Short-Term Memory (LSTM) models, when integrated with Sentinel-2 satellite imagery, accurately predict wheat yield, highlighting the value of combining

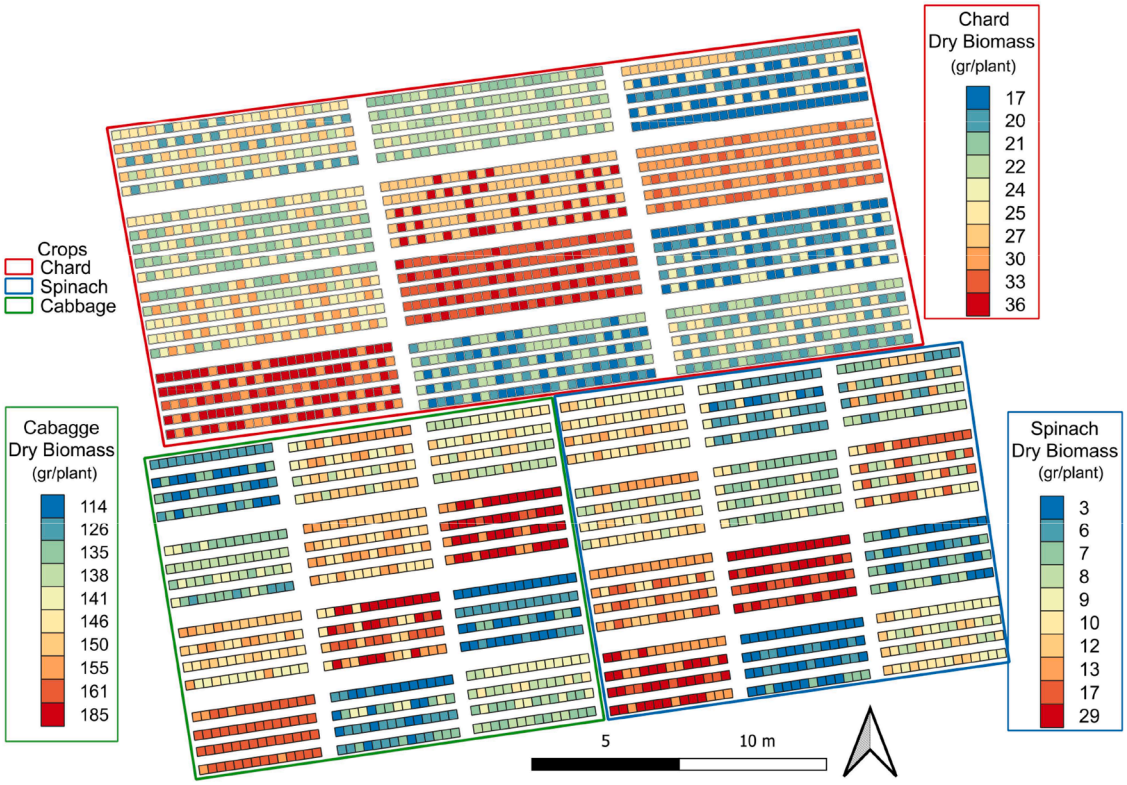

Fig. 7. Spatial prediction of vegetable crop yield using the best models.

remote sensing with advanced algorithms.

Further supporting these findings, Hu et al. (2025); and Silva et al. (2025) reported SVM achieving high accuracy levels in predicting yields for potato, tomato, and rice crops, particularly when combined with spectral indices such as the Normalized Difference Vegetation Index (NDVI), the Enhanced Vegetation Index (EVI), and the Green Normalized Difference Vegetation Index (GNDVI). Additionally, Ccopi et al. (2024) emphasized SVM's advantages in scenarios with limited sample sizes—a condition comparable to this study. These collective findings confirm that machine learning approaches not only enhance yield estimation accuracy but also serve as robust strategies for agricultural decision-making under environmental variability and sustainable management conditions.

The results underscore these predictive models' capacity to capture treatment influences on yield while enabling spatial visualization of biochar effects across experimental plots. This geospatial representation both supports the statistical findings and provides a valuable tool for planning and managing organic fertilization strategies in horticultural crops.

5. Conclusions

This study demonstrates that guinea pig manure-derived biochar significantly enhances the agronomic performance of spinach, cabbage, and chard in a dose-dependent manner. The 30 t ha^{-1} application rate proved most effective, substantially improving foliar and root development while maximizing dry biomass accumulation. Agronomic characterization revealed statistically significant increases in key growth parameters—including number of leaves, leaf length, and dry weight—confirming biochar's considerable potential as an organic amendment for horticultural production systems in high Andean regions.

The successful integration of spectral and agronomic variables through advanced machine learning algorithms yielded highly accurate crop yield predictions, with the Support Vector Machine (SVM) model excelling for spinach cultivation, while Classification and Regression Trees (CART) models demonstrated superior performance for chard and cabbage. These findings validate the feasibility and effectiveness of implementing digital agriculture approaches to optimize biochar management practices and support evidence-based agronomic decision-making processes. Future research should evaluate biochar performance across different phenological stages and seasonal conditions, while expanding applications to demonstrate plots with diverse crop varieties. Further integration of spectral and agronomic variables will enable more comprehensive and nuanced evaluation protocols, ultimately facilitating the effective validation of biochar applications under extensive agricultural production conditions. This integrated approach promises to advance sustainable agricultural practices in high-altitude growing regions while providing data-driven frameworks for optimizing organic amendment strategies.

Ethics statement

Not applicable: This manuscript does not include human or animal research.

Funding

This research was funded by the INIA project "Mejoramiento de los servicios de investigación y transferencia tecnológica en el manejo y recuperación de suelos agrícolas degradados y aguas para riego en la pequeña y mediana agricultura en los departamentos de Lima, Áncash, San Martín, Cajamarca, Lambayeque, Junín, Ayacucho, Arequipa, Puno y Ucayali" CUI 2487112, of the Ministry of Agrarian Development and Irrigation (MIDAGRI) of the Peruvian Government.

CRediT authorship contribution statement

Dennis Ccopi: Writing – review & editing, Visualization, Software, Methodology, Investigation, Formal analysis, Conceptualization. **Edilson Requena-Rojas:** Writing – original draft, Visualization, Validation, Software, Methodology. **Alberto Arias-Arredondo:** Validation, Software, Methodology, Formal analysis, Data curation. **Maglorio Taipe:** Writing – review & editing, Writing – original draft, Validation, Conceptualization. **Jhonny Marcelo:** Writing – original draft, Visualization, Validation, Conceptualization. **Samuel Pizarro:** Writing – review & editing, Visualization, Software, Methodology, Investigation, Formal analysis, Conceptualization.

Declaration of competing interest

The authors declare that they have no known competing financial interests or personal relationships that could have appeared to influence the work reported in this paper.

Acknowledgments

We would like to express our deepest gratitude to everyone who contributed to this research at the Santa Ana Experimental Station – Huancayo.

Data availability

Data will be made available on request.

References

Abbruzzini, T.F., Davies, C.A., Toledo, F.H., Cerri, C.E.P, 2019. Dynamic biochar effects on nitrogen use efficiency, crop yield and soil nitrous oxide emissions during a tropical wheat-growing season. J. Environ. Manage 252, 109638. https://doi.org/10.1016/j.jenvman.2019.109638.

Ansarifar, J., Wang, L., Archontoulis, S.V., 2021. An interaction regression model for crop yield prediction. Sci. Rep. 11, 17754. https://doi.org/10.1038/s41598-021-97221-7.

Bazrafkan, A., Worral, H., Bandillo, N., Flores, P., 2025. Accurate plant height estimation in pulse crops through integration of LiDAR, multispectral information, and machine learning. Remote Sens. Appl.: Soc. Environ. 37, 101517. https://doi.org/10.1016/j.rsase.2025.101517.

Canatoy, R.C., Cho, S.R., Ok, Y.S., Jeong, S.T., Kim, P.J., 2022. Critical evaluation of biochar utilization effect on mitigating global warming in whole rice cropping boundary. Sci. Total Environ. 827, 154344. https://doi.org/10.1016/j.scitotenv.2022.154344.

Cao, H., Zhao, R., Xia, L., Wu, S., Yang, P., 2025. Trends in crop yield estimation via data assimilation based on multi-interdisciplinary analysis. Field. Crops. Res. 322, 109745. https://doi.org/10.1016/j.fcr.2025.109745.

Ccopi, D., Ortega, K., Castañeda, I., Rios, C., Enriquez, L., Patricio, S., Ore, Z., Casanova, D., Agurto, A., Zuñiga, N., Urquizo, J., 2024. Using UAV images and phenotypic traits to predict potato morphology and yield in Peru. Agriculture 14, 1876. https://doi.org/10.3390/agriculture14111876.

Cárdenas, F.L., 2025. Guinea pig breeding, consumption, prices, and exports in Peru: what do the statistical sources say? J. Bus. 16, 101–129. https://doi.org/10.21678/jb.2025.2388.

Davidson, C., Jaganathan, V., Sivakumar, A.N., Czarnecki, J.M.P., Chowdhary, G., 2022. NDVI/NDRE prediction from standard RGB aerial imagery using deep learning. Comput. Electron. Agric. 203, 107396. https://doi.org/10.1016/J.COMPAG.2022.107396.

Dayil, J.L., Akande, O., Mahmoud, A.E.D., Kimera, R., Omole, O., 2025. Challenges and opportunities in machine learning for bioenergy crop yield prediction: a review. Sustain. Energy Technol. Assess. 73, 104057. https://doi.org/10.1016/j.seta.2024.104057.

Egbeagu, U.U., Liu, W., Zhang, J., Sun, L., Bello, A., Wang, B., Deng, L., Sun, Y., Han, Y., Zhao, Y., Zhao, L., Zhao, M., Bi, R., Jong, C., Shi, S., Xu, X., 2023. The activity of ammonia-oxidizing bacteria on the residual effect of biochar-compost amended soils in two cropping seasons. Biochem. Eng. J. 191, 108778. https://doi.org/10.1016/j.bej.2022.108778.

Eghlima, G., Mohammadi, M., Aghamir, F., 2025. Biochar application improved soil properties, growth performances, essential oil, and rosmarinic acid content of *Thymus vulgaris L.* under salt stress. Plant Physiol. Biochem. 222 (January), 109698. https://doi.org/10.1016/j.plaphy.2025.109698.

Gade, S.A., Madolli, M.J., García-Caparrós, P., Ullah, H., Cha-um, S., Datta, A., Himanshu, S.K., 2025. Advancements in UAV remote sensing for agricultural yield estimation: a systematic comprehensive review of platforms, sensors, and data

analytics. Remote Sens. Appl.: Soc. Environ. 37, 101418. https://doi.org/10.1016/j.rsase.2024.101418.
Gao, Y., Shao, G., Lu, J., Zhang, K., Wu, S., Wang, Z., 2020. Effects of biochar application on crop water use efficiency depend on experimental conditions: a meta-analysis. Field. Crops. Res. 249. https://doi.org/10.1016/j.fcr.2020.107763.
Garcia, G., Treccarichi, S., Calì, R., Arena, D., Tribulato, A., Branca, F., 2025. Nitrogen use efficiency of microbial and amino acid treatments for organic broccoli (*Brassica oleracea L. var. italica Plenk*) seed production. Horticulturae 11, 253. https://doi.org/10.3390/horticulturae11030253.
Gelardi, D.L., Lazicki, P.A., Rath, D., Leinfelder-Miles, M.M., Scow, K.M., Geisseler, D.J., Parikh, S.J., 2025. Three-year field trials with seven biochars reveal minor changes in soil chemical properties but no impact on crop yield. Field. Crops. Res. 32, 109807. https://doi.org/10.1016/j.fcr.2025.109807.
Ghazouani, H., Ibrahimi, K., Amami, R., Helaoui, S., Boughattas, I., Kanzari, S., Milham, P., Ansar, S., Sher, F., 2023. Integrative effect of activated biochar to reduce water stress impact and enhance antioxidant capacity in crops. Sci. Total Environ. 905, 166950. https://doi.org/10.1016/j.scitotenv.2023.166950.
Grandgirard, J., Poinsot, D., Krespi, L., Nénon, J.P., Cortesero, A.M., 2002. Costs of secondary parasitism in the facultative hyperparasitoid Pachycrepoideus dubius: does host size matter? Entomol. Exp. Appl. 103 (3), 239–248. https://doi.org/10.1023/A.
Guo, Y., Samson, V.M., Zhi, Y., Chen, Y., Yang, X., Jia, G., Mao, Y., 2025. Biochar-fertilizer interaction increases nitrogen retention, uptake and use efficiency of cinnamomum camphora: a 15N tracer study. Geoderma Reg. 40 (February), e00936. https://doi.org/10.1016/j.geodrs.2025.e00936.
Hall, D.J.M., Bell, R.W., 2015. Biochar and compost increase crop yields but the effect is short term on sandplain soils of western australia. Pedosphere 25, 720–728. https://doi.org/10.1016/S1002-0160(15)30053-9.
Hernández-Huerta, J., Guerrero, B.I., Acevedo-Barrera, A.A., Balandrán-Valladares, M.I., Yañez-Muñoz, R.M., De Dios-Avila, N., Gutiérrez-Chávez, A., 2025. Biostimulant effects of trichoderma asperellum in hydroponic spinach production. Life 15, 428. https://doi.org/10.3390/life15030428.
Hidayaturrohman, Q.A., Hanada, E., 2025. A comparative analysis of hyper-parameter optimization methods for predicting heart failure outcomes. Appl. Sci. 15, 3393. https://doi.org/10.3390/app15063393.
Hu, H., Meng, J., Zheng, H., Cai, H., Wang, M., Luo, Z., E, Y., Li, C., Wu, Q., Yan, Z., Lei, Y., 2024. Relief effect of biochar on continuous cropping of tobacco through the reduction of p-hydroxybenzoic acid in soil. Heliyon 10, e33011. https://doi.org/10.1016/j.heliyon.2024.e33011.
Hu, J., Du, X., Li, Q., Zhang, Y., Wang, H., Xu, J., Xiao, J., Shen, Y., Dong, Y., Hu, H., Yan, S., Gong, S., 2025. Aboveground biomass estimation of highland barley in Qinghai–Tibet Plateau—Exploring the advantages of time series data and terrain effects. Remote Sens. 17, 655. https://doi.org/10.3390/rs17040655.
Hu, Y., Sun, B., Wu, S., Feng, H., Gao, M., Zhang, B., Liu, Y., 2021. After-effects of straw and straw-derived biochar application on crop growth, yield, and soil properties in wheat (*Triticum aestivum* L.) -maize (*Zea mays* L.) rotations: a four-year field experiment. Sci. Total Environ. 780. https://doi.org/10.1016/j.scitotenv.2021.146560.
Huete, A.R., 1988. A soil-adjusted vegetation index (SAVI) 295. Remote Sens. Environ. 25.
Husson, A.F., Josse, J., Le, S., Mazet, J., & Husson, M.F. (2025). *Package ' FactoMineR'*.
Isaza, C., Aleman-trejo, A.M., Ramirez-gutierrez, C.F., Rizzo-sierra, J.A., Anaya, K., Paul, J., & Paz, Z.De. (2025). *Spinach (Spinacia oleracea L .) growth model in indoor controlled environment using agriculture 4 . 0*. 1–24.
Ishaq, R.A.F., Zhou, G., Jing, G., Shah, S.R.A., Ali, A., Imran, M., Jiang, H., Obaid-ur-Rehman, 2025. Geospatial robust wheat yield prediction using machine learning and integrated crop growth model and time-series satellite data. Remote Sens. 17 (7), 1140. https://doi.org/10.3390/rs17071140.
Jabed, M.A., Azmi Murad, M.A., 2024. Crop yield prediction in agriculture: a comprehensive review of machine learning and deep learning approaches, with insights for future research and sustainability. Heliyon 10 (24), e40836. https://doi.org/10.1016/j.heliyon.2024.e40836.
Jaufmann, E., Schmid, H., Hülsbergen, K.J., 2024. Effects of biochar in combination with cattle slurry and mineral nitrogen on crop yield and nitrogen use efficiency in a three-year field experiment. Eur. J. Agron. 156. https://doi.org/10.1016/j.eja.2024.127168.
Jha, S., Gaur, R., Shahabuddin, S., Tyagi, I., 2023. Biochar as sustainable alternative and green adsorbent for the remediation of noxious pollutants: a comprehensive review. In: Toxics, 11. MDPI. https://doi.org/10.3390/toxics11020117.
Jhajharia, K., Mathur, P., 2023. Prediction of crop yield using satellite vegetation indices combined with machine learning approaches. Adv. Space Res. 72 (9), 3998–4007. https://doi.org/10.1016/j.asr.2023.07.006.
Jiang, Y., Li, T., Xu, X., Sun, J., Pan, G., Cheng, K., 2024b. A global assessment of the long-term effects of biochar application on crop yield. In: Current Research in Environmental Sustainability, 7. Elsevier B.V. https://doi.org/10.1016/j.crsust.2024.100247
Jiang, Z., Huete, A.R., Didan, K., Miura, T., 2008. Development of a two-band enhanced vegetation index without a blue band. Remote Sens. Environ. 112 (10), 3833–3845. https://doi.org/10.1016/J.RSE.2008.06.006.
Jiang, T.-J., Morgan, H.M., Tsai, W.-T., 2024a. Optimization of vertical fixed-bed pyrolysis for enhanced biochar production from diverse agricultural residues. Materials 17, 3030. https://doi.org/10.3390/ma17123030.
Karlsson, M., Jönsson, H.L., Hultberg, M., 2025. Inclusion of biochar in mushroom substrate influences microbial community composition of the substrate and elemental composition of the fruiting bodies. Sci. Total Environ. 968 (February). https://doi.org/10.1016/j.scitotenv.2025.178914.
Knez, M., Mattas, K., Gurinovic, M., Gkotzamani, A., Koukounaras, A., 2024. Revealing the power of green leafy vegetables: cultivating diversity for health, environmental benefits, and sustainability. In: Global Food Security, 43. Elsevier B.V. https://doi.org/10.1016/j.gfs.2024.100816
Legates, D.R., McCabe, G.J., 1999. Evaluating the use of "goodness-of-fit" measures in hydrologic and hydroclimatic model validation. Water. Resour. Res. 35 (1), 233–241. https://doi.org/10.1029/1998WR900018.
Levy, M. (2024). *Package ' corrplot'*.
Lin, G., Wang, Y., Wu, X., Meng, J., Ok, Y.S., Wang, C.H., 2025. Enhancing agricultural productivity with biochar: evaluating feedstock and quality standards. Bioresour. Technol. Rep. 29 (August 2024), 102059. https://doi.org/10.1016/j.biteb.2025.102059.
Liu, H., Dou, W., Zhang, W., Shi, G., Li, Y., Wang, L., 2025a. Coapplication of biochar and nitrogen fertilizer affects soybean yield by regulating the microbiome and metabolite profile of rhizosphere soil. Rhizosphere 33 (August 2024), 101019. https://doi.org/10.1016/j.rhisph.2025.101019.
Liu, H.Q., Huete, A., 1995. A feedback based modification of the NDVI to minimize canopy background and atmospheric noise. IEEE Trans. Geosci. Remote Sens. 33 (2).
Liu, Y., Liu, Y., Zhang, A., Yang, C., Wang, Y., Zhou, H., Yang, S., Tang, J., Sun, J., Liu, Y., 2025b. Behavior and mechanism of perfluorooctane sulfonate (PFOS) removal from wastewater samples using bamboo powder biochar. J. Water. Process. Eng. 70, 107102. https://doi.org/10.1016/j.jwpe.2025.107102.
Luna-Garcia, L.R., Robledo-Torres, V., Gonzalez-Cortes, A., Mendoza-Villarreal, R., Paredes-Jacome, J.R., 2023. Effect of pepper rootstocks as a sustainable alternative to improve yield and fruit quality. Horticulturae 9, 795. https://doi.org/10.3390/horticulturae9070795.
Marazza, D., Pesce, S., Greggio, N., Vaccari, F.P., Balugani, E., Buscaroli, A., 2022. The long-term Experiment Platform for the study of agronomical and environmental effects of the biochar: methodological Framework. Agriculture 12, 244. https://doi.org/10.3390/agriculture12081244.
Max, A., Wing, J., Weston, S., Williams, A., Keefer, C., Engelhardt, A., Cooper, T., Mayer, Z., Ziem, A., Scrucca, L., Hunt, T., & Kuhn, M.M. (2024). *Package ' caret'*.
Mishra, R.K., Chinnam, S., Sharma, A., 2025. Thermocatalytic pyrolysis of low-value waste biomass: thermal decomposition, kinetics behaviour, and biochar characterization. Results. Eng. 25, 104210. https://doi.org/10.1016/J.RINENG.2025.104210.
Morán-Figueroa, G.H., Muñoz-Pérez, D.F., Rivera-Ibarra, J.L., Cobos-Lozada, C.A., 2024. Model for predicting maize crop yield on small farms using clusterwise linear regression and GRASP. Mathematics 12 (21). https://doi.org/10.3390/math12213356.
Morshed, S., Barua, F., Khanom, A., Lokman, F., Zubair, H.T., 2025. Smart Agricultural Technology crop yield prediction using machine learning : an extensive and systematic literature review. Smart Agric. Technol. 10, 100718. https://doi.org/10.1016/j.atech.2024.100718.
Nassary, E.K., 2025. Biochar from maize cob waste : a path to carbon sequestration, enhancing soil health, maize productivity, and climate resilience in Tanzania. Next Res. 2, 100229. https://doi.org/10.1016/j.nexres.2025.100229.
Ortiz-Liébana, N., Zotti, M., Barquero, M., González-Andrés, F., 2023. Biochar + AD exerts a biostimulant effect in the yield of horticultural crops and improves bacterial biodiversity and species richness in the rhizosphere. Sci. Hortic. 321, 112277. https://doi.org/10.1016/j.scienta.2023.112277.
Picado, E.F., & Romero, K.F. (2025). *Mapping spatial variability of sugarcane foliar nitrogen, phosphorus, potassium and chlorophyll concentrations using remote sensing*. i, 1–19.
Qayyum, M.F., Haider, G., Raza, M.A., Mohamed, A.K.S.H., Rizwan, M., El-Sheikh, M.A., Alyemeni, M.N., Ali, S., 2020. Straw-based biochar mediated potassium availability and increased growth and yield of cotton (Gossypium hirsutum L.). J. Saudi Chem. Soc. 24, 963–973. https://doi.org/10.1016/J.JSCS.2020.10.004.
Ren, S., Zhong, J., Wang, K., Liu, R., Feng, H., Dong, Q., Yang, Y., 2025. Application of biochar in saline soils enhances soil resilience and reduces greenhouse gas emissions in arid irrigation areas. Soil Tillage Res. 250, 106500. https://doi.org/10.1016/j.still.2025.106500.
Santos, D.C.B.D., Evaristo, R.B.W., Dutra, R.C., Suarez, P.A.Z., Silveira, E.A., Ghesti, G.F., 2025. Advancing biochar applications: a review of production processes, analytical methods, decision criteria, and pathways for scalability and certification. Sustainability 17, 2685. https://doi.org/10.3390/su17062685.
Senamhi, 2020. Climas del Perú Mapa de Cllasificación Climática Nacional. In: Ministerio Del Ambiente, 53.
Sharma, I.K., Di Prima, S., Essink, D., Broerse, J.E.W., 2021. Nutrition-sensitive agriculture: a systematic review of impact pathways to Nutrition outcomes. In: Advances in Nutrition, 12. Oxford University Press, pp. 251–275. https://doi.org/10.1093/advances/nmaa103.
Silva, P.C., Sabino, M.B., Ferreira, M.B., Sabino, N.C.O., Sousa, L.S., Elias, M.B., Silva, A. B., Ferreira, A.F.A., Costa, A.R., Delmond, J.G., Silva, J.L.B., Oliveira, H.F.E., Silva, T.G.F., Silva, M.V., 2025. Agronomic effects of different rock powder rates associated with irrigation water depths: potential for lettuce (*Lactuca sativa* L.) production. Agriculture 15, 663. https://doi.org/10.3390/agriculture15060663.
Song, J., Huang, J., Huang, H., Xiao, G., Li, X., Li, L., Su, W., Wu, W., Yang, P., Liang, S., 2024. Improving crop yield estimation by unified model parameters and state variable with bayesian inference. Agric. For. Meteorol. 355, 110101. https://doi.org/10.1016/j.agrformet.2024.110101.
Taweengern, K., Thapsamut, T., Khaobang, C., Areeprasert, C., Aramrak, S., 2025. Circular utilization of sugarcane bagasse for water and nutrient retention in two-type of sugarcane cultivation soil by biochar and hydrochar addition. Fuel 392, 134870. https://doi.org/10.1016/j.fuel.2025.134870.

Trentin, C., Ampatzidis, Y., Lacerda, C., Shiratsuchi, L., 2024. Tree crop yield estimation and prediction using remote sensing and machine learning: a systematic review. Smart Agric. Technol. 9, 100556. https://doi.org/10.1016/j.atech.2024.100556.

Villegas-camacho, O., Francisco-valencia, I., & Alejo-eleuterio, R. (2025). *FTIR-based microplastic classification : a comprehensive study on normalization and ML techniques*. 1–20.

Wang, Y., Miao, H., Zhang, F., & Sun, B. (2025). *Seasonal variation in nutritional substances in varieties of leafy Chinese kale (Brassica oleracea var . alboglabra): a pilot trial*. 1–16.

Wickham, H., Vaughan, D., & Girlich, M. (2024). *tidyr: tidy Messy Data. R package version 1.3.1*.

Xu, H., Cai, A., Wu, D., Liang, G., Xiao, J., Xu, M., Colinet, G., Zhang, W., 2021. Effects of biochar application on crop productivity, soil carbon sequestration, and global warming potential controlled by biochar C:n ratio and soil pH: a global meta-analysis. Soil Tillage Res. 213, 105125. https://doi.org/10.1016/j.still.2021.105125.

Xu, P., Sun, C.X., Ye, X.Z., Xiao, W.D., Zhang, Q., Wang, Q., 2016. The effect of biochar and crop straws on heavy metal bioavailability and plant accumulation in a Cd and Pb polluted soil. Ecotoxicol. Environ. Saf. 132, 94–100. https://doi.org/10.1016/j.ecoenv.2016.05.031.

Xue, J., Huete, A., Liu, Z., Gao, S., Lu, X., 2025. A lightweight SIF-based crop yield estimation model: a case study of Australian wheat. Agric. For. Meteorol. 364, 110439. https://doi.org/10.1016/j.agrformet.2025.110439.

Yan, S., Wang, P., Cai, X., Wang, C., Van Zwieten, L., Wang, H., Yin, Q., Liu, G., Ren, T., 2025. Biochar-based fertilizer enhanced tobacco yield and quality by improving soil quality and soil microbial community. Environ. Technol. Innov. 37, 103964. https://doi.org/10.1016/j.eti.2024.103964.

Ye, Z., Zhai, X., She, T., Liu, X., Hong, Y., Wang, L., Zhang, L., Wang, Q., 2024. winter wheat yield prediction based on the ASTGNN Model coupled with multi-source data. Agronomy 14, 2262. https://doi.org/10.3390/agronomy14102262.

Zhang, L., Yao, Z., Zhao, L., Yu, F., Li, Z., Yi, W., Fu, P., Jia, J., Zhao, Y., 2024. Effects of various pyrolysis temperatures on the physicochemical characteristics of crop straw-derived biochars and their application in tar reforming. Catal. Today 433, 115663. https://doi.org/10.1016/j.cattod.2024.114663.

Zhang, P., Lu, B., Ge, J., Wang, X., Yang, Y., Shang, J., La, Z., Zang, H., Zeng, Z., 2025. Using UAV-based multispectral and RGB imagery to monitor above-ground biomass of oat-based diversified cropping. Eur. J. Agron. 162, 127422. https://doi.org/10.1016/j.eja.2024.127422.

Zhang, Q., Song, Y., Wu, Z., Yan, X., Gunina, A., Kuzyakov, Y., Xiong, Z., 2020. Effects of six-year biochar amendment on soil aggregation, crop growth, and nitrogen and phosphorus use efficiencies in a rice-wheat rotation. J. Clean. Prod. 242, 118435. https://doi.org/10.1016/j.jclepro.2019.118435.